NIH Public Access
Author Manuscript
*J Immunol*. Author manuscript; available in PMC 2014 October 15.

Published in final edited form as:
*J Immunol*. 2013 October 15; 191(8): 4038–4047. doi:10.4049/jimmunol.1301282.

# Fatal eosinophilic myocarditis develops in the absence of IFNγ and IL17A

**Jobert G. Barin**[1,2,3], **G. Christian Baldeviano**[3,4], **Monica V. Talor**[2], **Lei Wu**[3], **SuFey Ong**[3], **DeLisa Fairweather**[5], **Djahida Bedja**[6], **Natalie R. Stickel**[7], **Jillian A. LeGault**[3], **Ashley B. Cardamone**[2], **Dongfeng Zheng**[2], **Kathleen L. Gabrielson**[6], **Noel R. Rose**[1,2,3], and **Daniela Cihakova**[2]

[1]Immunology Training Program, The Johns Hopkins University School of Medicine, Baltimore, MD 21205

[2]Dept. of Pathology, The Johns Hopkins University School of Medicine

[3]The William H. Feinstone Dept. of Molecular Microbiology & Immunology, The Johns Hopkins University Bloomberg School of Public Health

[4]Dept. of Parasitology, US Naval Medical Research Unit Six (NAMRU-6), Lima, Peru

[5]Dept. of Environmental Health Sciences, The Johns Hopkins University Bloomberg School of Public Health

[6]Dept. of Comparative Medicine, The Johns Hopkins University School of Medicine

[7]Dept. of Hematology & Oncology, University of Freiburg, Freiburg, Germany

## Abstract

$CD4^+$ T cells play a central role in inflammatory heart disease, implicating a cytokine product associated with helper T cell effector function as a necessary mediator of this pathophysiology. IFNγ-deficient mice developed severe autoimmune myocarditis (EAM), in which mice are immunized with cardiac myosin peptide, while IL17A-deficient mice were protected from progression to dilated cardiomyopathy. We generated $IFN\gamma^{-/-}IL17A^{-/-}$ mice to assess whether IL17 signaling was responsible for the severe EAM of $IFN\gamma^{-/-}$ mice. Surprisingly, $IFN\gamma^{-/-}IL17A^{-/-}$ mice developed a rapidly fatal EAM. Eosinophils comprised a third of infiltrating leukocytes, qualifying this disease eosinophilic myocarditis. We found increased cardiac production of CCL11/eotaxin, and Th2 deviation among heart-infiltrating $CD4^+$ cells. Ablation of eosinophil development improved survival of $IFN\gamma^{-/-}IL17A^{-/-}$ mice, demonstrating the necessity of eosinophils in fatal heart failure. The severe and rapidly fatal autoimmune inflammation that developed in the combined absence of IFNγ and IL17A constitutes a novel model of eosinophilic heart disease in humans. This is also the first demonstration that eosinophils have the capacity to act as necessary mediators of morbidity in an autoimmune process.

### Keywords

myocarditis; autoimmune disease; cytokines; IFNγ; IL17A; eosinophils; Th2 cells

Corresponding author: Daniela Cihakova, MD PhD – dcihako1@jhmi.edu, Ross 648, 720 Rutland Ave., Baltimore, MD 21205-2196.

**Disclosures:** None

NIH-PA Author Manuscript
NIH-PA Author Manuscript
NIH-PA Author Manuscript

NIH-PA Author Manuscript

NIH-PA Author Manuscript

NIH-PA Author Manuscript

## Introduction

Myocarditis encompasses a diverse family of inflammatory heart diseases associated with a large variety of infectious and pharmacologic etiologies. (1, 2) We have published extensively on myocarditis as a paradigm of post-infectious autoimmunity, where autoaggressive responses represent a critical intermediate in the development of lasting cardiologic sequelae, often culminating in inflammatory dilated cardiomyopathy (DCM) and heart failure. (3–5) Myocarditis can take several phenotypic forms in humans, including necrotizing eosinophilic myocarditis, a variant associated with poor prognosis and rapidly fatal outcomes. (6–8)

Experimental autoimmune myocarditis (EAM) is a model of human inflammatory heart disease in which animals are immunized with cardiac antigens to recapitulate autoreactive responses following viral clearance. (9, 10) The disease is dependent on $CD4^+$ T cells, implicating cytokine products of these cells as necessary signaling intermediaries in disease pathophysiology (11).

Interleukin-17 (IL17) has been described as a family of proinflammatory cytokines bridging innate and adaptive immunity (12). We recently reported a critical requirement for IL17A in mediating profibrotic remodeling in the heart during EAM and subsequent progression to DCM; whereas $IL17A^{-/-}$ mice are protected from fibrosis, they are not protected from inflammatory myocarditis. (13) The archetypal member of this family, IL17A, elicits neutrophilic responses in host defense to fungi and extracellular bacteria. (14, 15) IL17 signaling pathways bear phylogenetic and signaling relationships to the TLR/IL1 superfamily. (16) Immunologically relevant production of IL17A has been identified in various cellular populations, including γδ T cells, NK cells, and a subset of $CD4^+$ T cells, termed “Th17” cells. (17, 18) Th17 differentiation is programmed by coordinate signaling from TGFβ, IL6, and IL23, and is dependent on the transcription factor retinoic acid receptor-related orphan receptor gamma (RORγt). (19, 20)

The involvement of Th17 $CD4^+$ cells in autoimmune disease continues to be an active area of investigation. The importance of the Th17 lineage was discovered, in part, by contrasting the roles of IL23 and IL12 in the pathogenesis of experimental autoimmune encephalomyelitis (EAE). (21) Adoptive transfer experiments have shown that Th17-conditioned cells induced qualitatively different, if not more severe, autoimmune pathology than Th1 cells. (22–24)

$IFN\gamma^{-/-}$ mice develop more severe EAM than wild type (WT) controls, and progress to fibrosis and DCM at later timepoints. (25–28) Th17 lineage cells are thought to be responsible for the protective effect of IFNγ in several animal models of autoimmune disease. (29, 30) More severe disease may be elicited in $IFN\gamma^{-/-}$ mice through unconstrained outgrowth of autoaggressive Th17 clones *in vivo*. Several investigators have reported increased Th17 responses in association with severe disease in $IFN\gamma^{-/-}$ mice, consistent with this hypothesis. (31–35) These findings led us to investigate whether the protective effect of IFNγ in EAM is mediated through suppressing Th17 differentiation in autoaggressive $CD4^+$ T cells.

Unexpectedly, we found that mice deficient in both IFNγ and IL17A developed a severe, rapidly fatal form of EAM, characterized by extensive eosinophilic infiltration, cardiomyocyte necrosis, thrombogenesis, with evidence of Th2 deviation and rapid decline of cardiac function. Comparisons to both $IL17A^{-/-}$ and $IFN\gamma^{-/-}$ mice suggest that both cytokines collaborate in the suppression of autoaggressive Th2 differentiation and eosinophilic cardiac infiltration. In this report, we demonstrate a requisite role for

NIH-PA Author Manuscript

NIH-PA Author Manuscript

NIH-PA Author Manuscript

eosinophils in effecting the rapid mortality of eosinophilic myocarditis. We further provide evidence of specific features of autoimmune pathophysiology independently mediated by eosinophils, and the Th2 effector program, respectively.

## Materials & Methods

### Mice

IL17A$^{-/-}$ founder mice were kindly provided by Yoichiro Iwakura (U. of Tokyo). IFN$\gamma^{-/-}$ and WT BALB/cJ mice were obtained from the Jackson Laboratory (Bar Harbor, ME). IL17A$^{-/-}$ mice were crossed to IFN$\gamma^{-/-}$, and bred to homozygosity at both loci employing established PCR genotyping. (36, 37) Established IFN$\gamma^{-/-}$IL17A$^{-/-}$ BALB/c mice were outcrossed to the ΔdblGATA1 BALB/c strain (JAX 5653), and resulting progeny intercrossed for a minimum of two generations to generate homozygous triple-mutant founders. As a result, cross intermediates did not include ΔdblGATA1×single knockout controls, which may be the focus of future studies. All mice were maintained in the Johns Hopkins University School of Medicine specific-pathogen free vivarium. Experiments were conducted on 6–12 week old male mice, and in compliance with the Animal Welfare Act, and the principles set forth in the *Guide for the Care and Use of Laboratory Animals*. (38) All methods and protocols were approved by the Animal Care and Use Committee of The Johns Hopkins University.

### Induction of EAM

For the induction of EAM, we employed the myocarditogenic peptide MyHC$\alpha_{614–629}$ (Ac-SLKLMATLFSTYASAD), (39) commercially synthesized by fMOC chemistry, and purified to a minimum of 90% by HPLC (Genscript). On days 0 and 7, mice received *sc* axillary installations of 50–100 μg of MyHC$\alpha_{614–629}$ peptide emulsified in CFA (Sigma) supplemented to 5 mg/mL of heat-killed *M. tb* strain H37Ra (Difco). On day 0, mice also received 500 ng of pertussis toxin *ip* (List Biologicals).

### Coxsackie viral infection

Male 6–8 week old mice were maintained under pathogen-free conditions in the animal facility at Johns Hopkins School of Medicine. Mice were inoculated *ip* with $10^3$ (PFU of heart-passaged CVB3 (containing CVB3 and cardiac myosin) diluted in sterile PBS on day 0. This autoimmune model of CVB3 myocarditis closely resembles EAM. (40) CVB3 (Nancy strain) was originally obtained from the American Type Culture Collection (ATCC, Manassas, VA) and grown in Vero cells (ATCC), as previously described. (41) Myocarditis was assessed at day 10 post infection, during the peak of acute inflammation.

### Assessment of EAM

Mice were most commonly evaluated for the development of EAM at the peak of disease on day 21. Heart tissues were fixed in SafeFix (Thermo Fisher Scientific). Tissues were embedded longitudinally, and 5 μm serial sections were cut and stained with hematoxylin and eosin, or Masson's Trichrome Blue (HistoServ). Myocarditis severity was evaluated by microscopic approximation of the percent area of myocardium infiltrated with inflammatory cells, fibrosis, and cardiomyocyte necrosis determined from five sections per heart according to the following scoring system: grade 0 – no inflammation; grade 1 - less than 10% of the heart section is involved; grade 2 - 10–30%; grade 3 - 30–50%; grade 4 - 50–90%; grade 5 - more than 90%. (9) Grading was performed by a minimum of two independent, blinded investigators and averaged.

NIH-PA Author Manuscript

NIH-PA Author Manuscript

NIH-PA Author Manuscript

### *In vitro* stimulation

Splenocytes from mice with EAM were Lymphocyte-selected (Cedarlane) into 1x HBSS. For MyHC$\alpha_{614–629}$-specific recall stimulations, $10^6$ responder splenocytes from mice with EAM were cultured in the presence of 10 μg/mL MyHC$\alpha_{614–629}$ in 48-well format for 72–96 hours, or unstimulated for control.

### Flow cytometry

Heart-infiltrating leukocytes were isolated from animals perfused for 3 min with 1x PBS + 0.5% FBS, and digested in GentleMACS C Tubes according to manufacturer's instructions (Miltenyi Biotec). Splenocytes were also extracted into single cell suspension in 1x PBS + 0.5% FBS, and RBCs lysed by <5 minute incubation in ACK lysis buffer (Biofluids). Prior to surface staining, viability was determined by LIVE/DEAD staining according to manufacturer's instructions (Molecular Probes). Cells were washed and FcγRII/III blocked with αCD16/32 (eBiosciences). Surface markers were stained with fluorochrome-conjugated mAbs (eBiosciences, BD Pharmingen, BioLegend). Samples were acquired on the LSR II quad-laser cytometer running FACSDiva 6 (BD Immunocytometry). Data were analyzed with FlowJo 7.6 (Treestar Software).

### ELISA

Supernatants from stimulated cells were stored at −80° C. For cardiac homogenates, tissues were snap frozen, stored at −80°C, homogenized in MEM + 2% FBS, and stored at −80°C until used in ELISA or Linco assays. Homogenate cytokine levels were normalized to wet heart weights prior to homogenization. Linco multiplex cytokine assays (Millipore) were used according to manufacturer's instructions, and acquired on a Luminex XMAP reader. Alternately, quantitative sandwich ELISA for supernatants were determined by colorimetric ELISA kits according to manufacturers' recommended protocols (R&D Systems, IBL). Total serum IgE was determined by sandwich ELISA (BD Biosciences).

### Realtime PCR

Tissue mRNA was extracted in TRIZOL (Invitrogen), quantitated by Nanodrop (Thermo Fisher), DNAse digested (Ambion), and amplified with iQ SYBR Green mastermix (Biorad) acquired on the MyiQ2 thermocycler (Biorad) running iQ5 software (Biorad). Synthetic oligonucleotides were commercially synthesized, purified, and assayed by mass spectroscopy (Integrated DNA Technologies). 250 pmol of each primer template (Supplemental Table I) were used for 2 μg cDNA template for each reaction. Reactions were run as individual primer pairs for individual animals. Data were analyzed by the $2^{-\Delta\Delta Ct}$ method of Livak, *et al*., (42) comparing threshold cycles first to *Hprt* expression in individual animals, then ΔCt of target genes in naïve WT BALB/c controls. Certain data are pseudolinearized, to depict downregulation ($2^{-\Delta\Delta Ct} < 1$) as $-2^{\Delta\Delta Ct}$.

### Hydroxyproline determination

Cardiac samples are weighed, then hydrolyzed in 12N HCl O/N @ 120° C. Samples are dried in 96-well format plates, then incubated with 50 mm Chloramine T (Sigma), followed by 1M dimethylaminobenzaldehyde (Sigma) against a 1–100 μg/mL standard curve of hydroxyproline (Sigma). Samples are read at 570 nm, and values normalized to starting sample mass. (43)

### Echocardiography

Trans-thoracic echocardiography was performed using the Acuson Sequoia C256 ultrasonic imaging system (Siemens). Conscious, depilated, previously trained mice were gently held

NIH-PA Author Manuscript

NIH-PA Author Manuscript

NIH-PA Author Manuscript

in a supine position. The heart was imaged in the two-dimensional (2-D) mode in the parasternal short axis view, and an M-mode cursor was positioned perpendicular to the interventricular septum (IVS) and the left ventricular posterior wall (LVPW) at the level of the papillary muscles. From M-mode, the wall thicknesses and chamber dimensions were measured. For each mouse, three to five values for each measurement were obtained and averaged for evaluation. The left ventricular (LV) end diastolic dimension (LVEDD), LV end systolic dimension (LVESD), interventricular septal wall thickness at end diastole (IVSD), and LV posterior wall thickness at end diastole (LVPWTED) were measured from a frozen M-mode tracing. Fractional shortening (%FS), ejection fraction (%EF), LV mass, and relative wall thickness were calculated from this parameters as previously described. (44)

### Statistics

Multiple group comparisons were performed by ANOVA, followed by the Tukey-Kramer and Bonferroni post-test (StatPlus). Group survival was determined by Mantel-Cox log rank (GraphPad Prism). Asterisks denote statistically significant comparisons to wild type.

## Results

### Concurrent ablation of IFNγ and IL17A reveals a protective effect of IL17A in inflammatory autoimmune heart disease

To test our original hypothesis that IL17 signaling mediates the severe pathology observed in IFNγ-deficient mice, we crossed an IL17A-null allele to the IFN$\gamma^{-/-}$ background, in order to generate IFN$\gamma^{-/-}$IL17A$^{-/-}$ double-knockout (DKO) mice. EAM was induced in DKO mice, IFN$\gamma^{-/-}$ single-knockout, IL17A$^{-/-}$ single-knockout, and WT controls by immunization with myocarditogenic peptide (MyHC$\alpha_{614–629}$) in CFA. As we previously reported, IFN$\gamma^{-/-}$ animals developed severe EAM, and IL17A$^{-/-}$ animals developed EAM of similar severity to wild type animals. (13, 27)

Unexpectedly, accelerated mortality was observed in IFN$\gamma^{-/-}$ IL17A$^{-/-}$ animals, beginning at day 14 *post-immunization* (Figure 1a). In contrast, IFN$\gamma^{-/-}$ mice died only at later timepoints, consistent with our previously published reports. (26) Across experiments, between 50–100% of all immunized male and female IFN$\gamma^{-/-}$IL17A$^{-/-}$ mice consistently died during this timeframe, in both male and female IFN$\gamma^{-/-}$IL17A$^{-/-}$ animals (*data not shown*). The survival of IFN$\gamma^{-/-}$IL17A$^{-/-}$ mice was significantly poorer than IFN$\gamma^{-/-}$ control animals by Kaplan-Meier log-rank estimates ($p < 0.001$). Moreover, IFN$\gamma^{-/-}$IL17A$^{-/-}$ mice had more severe cardiac inflammation at time of death than did IFN$\gamma^{-/-}$, or other control mice (Figure 1b).

The degree of severity of disease in IFN$\gamma^{-/-}$IL17A$^{-/-}$ mice was unprecedented for the EAM model. The majority of IFN$\gamma^{-/-}$IL17A$^{-/-}$ animals had such severe myocarditis that the tissue resembled secondary lymphoid tissue. Infiltrating cells included numerous mononuclear cells, as well as frequent polymorphonuclear cells (Figure 1c). We observed extensive pericardial inflammation and fibrosis, as well as extensive cardiomyocyte necrosis, endocarditis, intraatrial thrombosis, and the formation of ectopic lymphoid follicle-like structures throughout the myocardium (Supplemental Figure 1).

In parallel experiments, we investigated the response of IFN$\gamma^{-/-}$IL17A$^{-/-}$ mice (and appropriate single-knockout controls) to acute infection with coxsackievirus B3 (CVB3), a cardiotropic enterovirus that has been previously described as an important agent in the elicitation of myocarditis in humans, as well as mouse models. (45–47) Similar to the EAM model, IFNγ-deficient mice developed more severe cardiac inflammation following CVB3 infection. (48) At day 10 following infection, 2 of 13 IFN$\gamma^{-/-}$IL17A$^{-/-}$ mice had expired,

NIH-PA Author Manuscript

NIH-PA Author Manuscript

NIH-PA Author Manuscript

and remaining animals were moribund (Supplemental Figure 2a), whereas all mice of the control genotypes survived to this timepoint. The severity of histopathological cardiac inflammation was largely comparable across strains (Supplemental Figure 2b–c).

## IFNγ$^{-/-}$IL17A$^{-/-}$ mice rapidly develop rapidly compromised cardiac function, independent of cardiac fibrosis

Echocardiographic imaging of IFNγ$^{-/-}$ IL17A$^{-/-}$ mice at day 14 demonstrated greatly compromised cardiac function and dramatic loss of cardiac contractility, as evidenced by diminished fractional shortening and ejection fraction in IFNγ$^{-/-}$IL17A$^{-/-}$, but not IFNγ$^{-/-}$ mice at this early timepoint (Figure 2a). We did not observe overt signs of left ventricular dilation (Supplemental Figure 3); however, left ventricular end-systolic dimensions were increased in IFNγ$^{-/-}$IL17A$^{-/-}$ mice (Figure 2b), as was the resulting calculated left ventricular mass (Figure 2c).

Cardiac fibrosis was assessed at day 21 of EAM by staining with Masson's Trichrome Blue (Figure 3a). Total collagen content of hearts was assayed by quantitative determination of hydroxyproline content, demonstrating diminished fibrosis in IFNγ$^{-/-}$IL17A$^{-/-}$ mice, compared to IFNγ$^{-/-}$ mice (Figure 3b). Transcriptional regulation of fibrotic collagens in IFNγ$^{-/-}$IL17A$^{-/-}$ hearts was interrogated by realtime PCR. Similar patterns of expression were observed for collagens I and III (Figure 3b–c), as well as MMP2 and MMP3 (Supplemental Figure 3). Together, these data confirm our previous findings that IL17A drives cardiac fibrosis, whereas IFNγ counterregulates this remodeling process. (13) However, it makes such fibrotic dilative remodeling unlikely to mediate the severe, morbid heart disease of IFNγ$^{-/-}$IL17A$^{-/-}$ mice.

## Cellular mediators of severe EAM in IFNγ$^{-/-}$ IL17A$^{-/-}$ mice

In order to address mechanisms by which IL17A could protect mice from eosinophilic myocarditis, we performed comprehensive cytometric profiling of the cardiac infiltrate at the peak of EAM in surviving mice (Figure 4a). Among the IFNγ$^{-/-}$ IL17A$^{-/-}$ mice that survived to day 21, the total number of CD45$^{+}$ leukocytes was similar to that seen in IFNγ$^{-/-}$ animals (Figure 4b, left). Notably, increased neutrophil infiltration was observed in IFNγ$^{-/-}$ hearts at day 21 of EAM; however, this recruitment was abolished in IFNγ$^{-/-}$IL17A$^{-/-}$ mice (Figure 4b–d).

Eosinophils were most abundant in IFNγ$^{-/-}$IL17A$^{-/-}$ hearts at day 21 (Figure 4b–e). By examining the loss of light-scattering of heart-infiltrating eosinophils as an indicator of degranulation, (49) we observed more numerous degranulated eosinophils at day 12 of EAM in IFNγ$^{-/-}$IL17A$^{-/-}$ mice (*data not shown*). Together, these data led us to conclude that concurrent ablation of IL17A replaced the predominantly neutrophilic infiltrate of IFNγ$^{-/-}$ mice with eosinophils.

Quantitatively, the most substantial differences in cellular infiltration were observed among granuloid cell types, although we also found differences between IFNγ$^{-/-}$IL17A$^{-/-}$ mice and IFNγ$^{-/-}$ animals in infiltration with other cell types. IFNγ$^{-/-}$IL17A$^{-/-}$ hearts tended to be more infiltrated with F4/80$^{+}$CD11b$^{+}$ macrophages, as well as FcεRIα$^{hi}$ mast cells (Figure 4b, *data not shown*).

We examined the spleens and blood of naïve IFNγ$^{-/-}$IL17A$^{-/-}$ mice to determine whether these differences in infiltrating leukocyte populations represent preexisting disparities in the frequencies of these cell subsets prior to the induction of EAM. Comparing the spleens of unimmunized IFNγ$^{-/-}$IL17A$^{-/-}$ and IFNγ$^{-/-}$ mice, we did not observe differences in the number of eosinophils, regulatory T cells, or dendritic cells (*data not shown*). We also did

NIH-PA Author Manuscript

NIH-PA Author Manuscript

NIH-PA Author Manuscript

not find differences in numbers of effector T cells, NK cells, γδ T cells, monocytes, or B cells (*data not shown*). In the peripheral blood of naïve IFNγ$^{-/-}$IL17A$^{-/-}$ mice, we observed a modest increase in the proportion of eosinophils (Figure 6a). Upon mock-immunization with PBS/CFA, IFNγ$^{-/-}$IL17A$^{-/-}$ mice did not develop peripheral eosinophilia, or eosinophilic cardiac infiltrates (*data not shown*). These data indicate that IFNγ$^{-/-}$IL17A$^{-/-}$ mice do not exhibit signs of general systemic eosinophilia. From this, we conclude that eosinophilic infiltration of the hearts of IFNγ$^{-/-}$IL17A$^{-/-}$ mice during EAM is specifically autoimmune, and not a generalized inflammatory disease of the IFNγ$^{-/-}$IL17A$^{-/-}$ strain.

## Eosinophilic mediators of severe EAM in IFNγ$^{-/-}$ IL17A$^{-/-}$ mice

In order to understand the differences in the recruitment of granulocytic effectors under coordinate control by IFNγ and IL17A, we examined the expression of a variety of cytokines, chemokines, and growth factors in the hearts and autoreactive T cells of IFNγ$^{-/-}$IL17A$^{-/-}$ and IFNγ$^{-/-}$ mice with EAM. As expected, chemokines, cytokines, and growth factors associated with Th17-dependent recruitment of neutrophils were largely downregulated in the absence of IL17, in a manner that did not track with cardiac disease (*data not shown*).

Eosinophil recruitment to sites of inflammation is largely mediated by chemokine utilization of the receptor CCR3 by the ligand CCL11/eotaxin-1. (50) Interrogation of cardiac homogenates of IFNγ$^{-/-}$IL17A$^{-/-}$ hearts during EAM demonstrated substantially greater production of CCL11/eotaxin-1 at day 12, and CCL24/eotaxin-2, compared to WT controls ($p < 0.001$) at day 21 (Figure 5a). No differences were detected in CCL26/eotaxin-3 expression at day 12; no expression was detectable at day 21 (*data not shown*). Altogether, these data indicate that IFNγ and IL17A collaborated in suppressing eosinophilic recruitment to the heart, via suppression of CCL11/eotaxin-1 and CCL24/eotaxin-2 production. We did not detect production of CCL11/eotaxin-1 from restimulated splenocyte cultures (*data not shown*), indicating its likely production by a non-hematopoietic, heart-resident cell type.

## Autoaggressive Th2 deviation in the severe EAM in IFNγ$^{-/-}$ IL17A$^{-/-}$ mice

Elevations in the expression of eotaxin CCR3 ligands implied deviation of autoreactive CD4$^+$ T cells to a Th2 phenotype. To further examine whether autoreactive IFNγ$^{-/-}$IL17A$^{-/-}$ CD4$^+$ cells were preferentially differentiating into Th2 cells at the single cell level, we performed intracellular staining for cytokines of heart-infiltrating CD4$^+$ T cells at day 12 of EAM. CD4$^+$ T cells staining for both IL4 and IL13 were increased in the hearts of IFNγ$^{-/-}$IL17A$^{-/-}$ mice, compared to the single-knockout controls, further confirming the expansion of autoaggressive CD4$^+$ cells with a Th2 phenotype in the combined absence of IFNγ and IL17A (Figure 5b–c). Together, these data indicate that autoreactive CD4$^+$ cells are constrained from Th2 differentiation by a synergistic actions of IFNγ and IL17. Intriguingly, this suppressive function appears to be preferentially targeted towards eosinophil-tropic functions of Th2 cells. It further implicates this eosinophilic Th2 deviation in the early mortality of IFNγ$^{-/-}$IL17A$^{-/-}$ EAM. In contrast, IL5 production in cardiac homogenates, cardiac transcripts, and restimulated splenocytes did not track with eosinophilia or disease in a cogent manner (*data not shown*). From these findings, we conclude that the collaborative suppression of cardiac eosinophilia by IFNγ and IL17A is mediated through eosinotropic chemokines that may be Th2-dependent, rather than through local or systemic expansion of eosinophils by IL5.

## Genetic ablation of eosinophils reverses the mortality of IFNγ$^{-/-}$IL17A$^{-/-}$ EAM

In order to demonstrate conclusively that eosinophils acted as requisite effectors of the severe, fatal cardiac pathology in the EAM of IFNγ$^{-/-}$IL17A$^{-/-}$ mice, we crossed onto this

NIH-PA Author Manuscript

NIH-PA Author Manuscript

NIH-PA Author Manuscript

background a mutated allele bearing a deletion of the high-affinity double-GATA binding site in the promoter of GATA1. This mutation selectively ablates differentiation of eosinophils, while leaving erythroid lineages unaffected. (51) The resulting triple-mutant ΔdblGATA1×IFNγ$^{-/-}$IL17A$^{-/-}$ mice showed fewer Siglec F$^{+}$Ly6G$^{int}$ eosinophils in peripheral blood (Figure 6a).

Upon induction of EAM, eosinophil-deficient triple-mutant mice were protected from the fatal heart failure observed in IFNγ$^{-/-}$IL17A$^{-/-}$ mice (Figure 6b). This protection was incomplete, as five of twenty-seven triple-mutant animals expired before the termination of the experiment on day 21; this survival rate approximately matches that of IFNγ$^{-/-}$ animals (Figure 1a, *not shown*). Statistically comparing ΔdblGATA1×IFNγ$^{-/-}$IL17A$^{-/-}$ and IFNγ$^{-/-}$IL17A$^{-/-}$ mice, Mantel-Cox logrank survival estimates were significantly different ($p = 0.0039$). We observed similar low rates of mortality in either male or female ΔdblGATA1×IFNγ$^{-/-}$IL17A$^{-/-}$ mice (*not shown*). Surprisingly, the severity of cardiac enlargement or inflammation did not differ between IFNγ$^{-/-}$IL17A$^{-/-}$ and ΔdblGATA1×IFNγ$^{-/-}$IL17A$^{-/-}$ mice (Figure 6c–d).

Cardiac function was assessed at day 15 by echocardiographic imaging. Consistent with their greater survival, ΔdblGATA1×IFNγ$^{-/-}$IL17A$^{-/-}$ mice had substantially improved cardiac function at this timepoint (Figure 6e). Functional improvement of fractional shortening and ejection fraction were largely due to diminished wall thickness parameters (IVSD, LVPWTED, LV mass, and relative wall thickness), rather than signs of ventricular dilation. Consistent with this observation, among the primary measurements in M-mode echocardiography (LVEDD, LVESD, IVSD, LVPWTED, heart rate), the thickness of the left ventricular posterior wall correlated best with the improved survival of ΔdblGATA1×IFNγ$^{-/-}$IL17A$^{-/-}$ mice (Figure 6f). Together, these data demonstrate that eosinophils are requisite mediators of the fatally severe myocarditis of IFNγ$^{-/-}$IL17A$^{-/-}$ mice in a manner by driving inflammatory hypertrophic cardiomyopathy.

## Discussion

We report here that in concert with IFNγ, IL17A exerts a protective effect in eosinophilic heart disease. IL17 has been ascribed protective functions in various other inflammatory pathologies, including CD45RB$^{hi}$ T cell transfer colitis, (52) DSS colitis, (53) and uveitis secondary to spondylarthropathy. (54) These results indicate that, in addition to anatomic considerations, IL17A exerts divergent pathophysiologic functions depending on the context of other cytokines.

The paradoxical protective effect of IFNγ in several models of autoimmune disease provide evidence that IFNγ can suppress disease pathology, contrary to the expected proinflammatory role of Th1 cells. This paradox had seemingly been resolved by the discovery of the Th17 lineage. IL23p19-deficient animals were protected from EAE, whereas IL12p35-deficient animals developed comparable disease to controls. (21)

We conclude from our prior experiments that the Th17 lineage prompts the pathogenesis of EAM. IL17A is the prototypic product of Th17 cells, which differentiate through a process requiring TGFβ, IL6, and IL23. (17, 18, 55) Although IL17A is not essential for the inflammatory process of EAM, it instead drives cardiac remodeling, fibrosis, and DCM development. (13) In WT mice, both Th1 and Th17 cells infiltrate the heart during EAM, but Th17 cells produce higher levels of inflammatory cytokines, such as TNFα, that have previously been shown to drive cardiac inflammation. (13) In addition, we have found that Th17-polarized cells are sufficient to transfer myocarditis (*unpublished results*). Our data remain consistent with the notion that Th17 cells mediate the severe disease of IFNγ$^{-/-}$

NIH-PA Author Manuscript

NIH-PA Author Manuscript

NIH-PA Author Manuscript

animals, as evidenced by enhanced neutrophil infiltration, as well as increased cardiac production of G-CSF and IL6 in IFNγ$^{-/-}$ mice (*data not shown*).

The myocarditic phenotype observed in IFNγ$^{-/-}$IL17A$^{-/-}$ mice is the most severe yet reported, even more so than the EAM of IFNγ$^{-/-}$, IFNγRI$^{-/-}$, or IL13$^{-/-}$ animals. (26, 44, 56) The rapid mortality begins at approximately day 14, shortly after the emergence of inflammatory cardiac lesions in WT mice, consistent with myocarditic process being the cause of death in IFNγ$^{-/-}$IL17A$^{-/-}$ animals. At this timepoint, we observed greater proportion of degranulating eosinophils, continuing to extensive eosinophilic infiltrates by day 21, where eosinophils comprise roughly a third of infiltrating cells. Most importantly, concurrent developmental ablation of eosinophils improved survival of IFNγ$^{-/-}$IL17A$^{-/-}$ mice.

Upstream of this fatal eosinophilic recruitment, we observed enhanced Th2 deviation in IFNγ$^{-/-}$IL17A$^{-/-}$ mice. Th2 deviation in IFNγ$^{-/-}$ mice corresponds to the classical Th1/Th2 model. (57) We have found novel evidence that IL17 signaling collaborates with IFNγ in the suppression of production of IL4, IL5, and IL13 by autoaggressive Th2 cells. While other Th2 and eosinophilic autoimmune disease models have been described, (58–65) to our knowledge this is the first that has been elicited by an intrinsically deviated response. Moreover, these data conclusively demonstrate a primary role for eosinophils in eliciting the rapid mortality of this deviated autoimmune response. The transcription factor Eomesodermin has recently been reported to be a critical regulator of this regulatory hierarchy among the Th2 cytokines, by selectively suppressing targeting of the Th2 transcription GATA3 to the *Il5* locus in memory Th2 cells. (66) These data provide novel evidence that IFNγ and IL17A are selectively collaborative in controlling eosinophilic effector functions of the Th2 response.

Importantly, we found evidence for pathophysiologic contributions of eosinophils that directly impact survival, which segregate away from effects on net cardiac inflammation. Eosinophil-deficient ΔdblGATA1×IFNγ$^{-/-}$IL17A$^{-/-}$ mice developed severe cardiac infiltrates and inflammation, comparable to IFNγ$^{-/-}$IL17A$^{-/-}$ mice, but did not die. Importantly, this protection observed in the triple-mutant genotype was associated with largely restored cardiac function, underscoring the important role of the eosinophil in mediating the death of IFNγ$^{-/-}$IL17A$^{-/-}$ mice. We are further undertaking studies employing triple-mutant mice to examine specific eosinophil chemotactic and effector pathways in mediating cardiotoxic mortality.

We interrogated a number of biomarkers to assess alternative deviation pathways that may contribute to the severe EAM of IFNγ$^{-/-}$IL17A$^{-/-}$ mice. We did not find compelling evidence for Tregs, Th9, non-classical Th17, or Th22 cells contributing to the disease phenotype of double-knockout mice (*data not shown*). We also did not find persuasive evidence of mast cell involvement in the disease pathology of IFNγ$^{-/-}$IL17A$^{-/-}$ mice. Despite the fact that more mast cells were detected in IFNγ$^{-/-}$IL17A$^{-/-}$ hearts, levels of intracardiac histamine and serum IgE did not track with disease (*data not shown*). While these data do not definitively rule out the participation of these pathways, they emphasize that eosinophilic Th2 deviation is primarily responsible for the severe, fatal disease of IFNγ$^{-/-}$IL17A$^{-/-}$ mice.

Among the types of myocarditis seen in patients, eosinophilic necrotizing myocarditis has one of the worst prognoses, often leading to rapid cardiac failure and death. (6, 67, 68) Most often, eosinophilic myocarditis in patients is seen as a sequela of eosinophilia-associated systemic pathology, in which infiltration is typically perivascular, with less profound damage to cardiomyocytes and better prognosis. (69) However, necrotizing eosinophilic

NIH-PA Author Manuscript

NIH-PA Author Manuscript

NIH-PA Author Manuscript

myocarditis may not be associated with increased numbers of peripheral eosinophils in the periphery. It progresses quickly, with severe eosinophilic infiltration in the myocardium, severe cardiomyocyte necrosis, intraventricular thrombi, and poor prognosis. (69–71) All of these features were observed as part of the necrotizing eosinophilic myocarditis in $IFN\gamma^{-/-}IL17A^{-/-}$ mice.

In a broader context, we can further envision that autoimmune diseases, as a whole, may be more heterogeneous than the Th17-centered view popularized since the discovery of the cell lineage. Th1 cells have been described to potentiate autoaggressive effector functions in several models, albeit to a generally lesser degree than Th17 cells. (22, 24, 72) Clearly, the pathogenicity of various cell lineages is linked to the location and inflammatory context of the model system in question. Our data argue for substantially greater redundancy among autoaggressive effector T cell subsets than has been previously appreciated.

It remains to be seen whether this redundancy is true for other autoimmune disease models. $IFN\gamma^{-/-}IL17A^{-/-}$ mice were not protected from EAE, nor did they develop accelerated disease. (73) This fundamental disjoint between EAE and EAM may reside in the fact that CNS lies behind the blood-brain barrier, and is historically regarded as a site of immune privilege. It is evident that different anatomic compartments possess different mechanisms to suppress inflammatory responses. Our data suggest that what we view as a predominantly Th1/Th17 response may be beneficial, insofar as it suppresses a potentially more devastating outcome. Because eosinophilic myocarditis is recognized as a distinct clinical entity with a particularly poor prognosis, our findings indicate that shared etiologic mechanisms may result in a qualitatively diverse spectrum of disease outcomes, depending on T cell polarization and downstream effector mechanisms involved.

These findings may have further implications for the deviation strategies entering clinical use as the first generation of IL12/23p40 antagonists are deployed for use in treating autoimmune disease. Caution may be warranted in investigational usage of these drugs in diseases with the potential for eosinophilic deviation.

## Supplementary Material

Refer to Web version on PubMed Central for supplementary material.

## Acknowledgments

The authors would like to extend their gratitude to R. Lee Blosser and Ada Tam for expert assistance with flow cytometric analysis methods; to Nicole Barat and the laboratories of J. Steven Dumler for assistance with multiplex cytokine analyses; to Norman J. Barker for expert assistance with photomicrography; to Yoichiro Iwakura for the generous provision of $IL17A^{-/-}$ founder animals; and to Patrizio Caturegli, Mark Lindsay, and Abdel Hamad for critical discussion and reading.

This work was supported by NIH/NHLBI grants R01 HL67290, R01 HL113008, and a Grant-in-Aid from the American Heart Association (to NRR). DF was supported by R01 HL087033. JGB has been the Mary Renner Fellow in Autoimmune Disease Research, and the O'Leary-Wilson Fellow at the Johns Hopkins Autoimmune Disease Research Center, from the American Autoimmune-Related Disease Association. DC is supported by The Michel Mirowski MD Discovery Foundation; the W.W. Smith Charitable Trust, heart research grant H1103; and The Children's Cardiomyopathy Foundation.

## References

1. Cihakova D, Rose NR. Pathogenesis of myocarditis and dilated cardiomyopathy. Adv Immunol. 2008; 99:95–114. [PubMed: 19117533]
2. Andreoletti L, Leveque N, Boulagnon C, Brasselet C, Fornes P. Viral causes of human myocarditis. Arch Cardiovasc Dis. 2009; 102:559–568. [PubMed: 19664576]

NIH-PA Author Manuscript

NIH-PA Author Manuscript

NIH-PA Author Manuscript


3. Afanasyeva, M.; Rose, NR. Viral infection and heart disease: autoimmune mechanisms. In: Shoenfeld, Y.; Rose, NR., editors. Infection and Autoimmunity. Elsevier; 2004. p. 299-318.
4. Rose, NR. Chronic Viral and Inflammatory Cardiomyopathy. Springer Verlag; 2005. The Significance of Autoimmunity in Myocarditis.
5. Eckart RE, Scoville SL, Campbell CL, Shry EA, Stajduhar KC, Potter RN, Pearse LA, Virmani R. Sudden death in young adults: a 25-year review of autopsies in military recruits. Ann Intern Med. 2004; 141:829–834. [PubMed: 15583223]
6. Ginsberg F, Parrillo JE. Eosinophilic myocarditis. Heart Fail Clin. 2005; 1:419–429. [PubMed: 17386864]
7. Cooper LT Jr. Myocarditis. The New England journal of medicine. 2009; 360:1526–1538. [PubMed: 19357408]
8. Magnani JW, Dec GW. Myocarditis: current trends in diagnosis and treatment. Circulation. 2006; 113:876–890. [PubMed: 16476862]
9. Cihakova D, Sharma RB, Fairweather D, Afanasyeva M, Rose NR. Animal models for autoimmune myocarditis and autoimmune thyroiditis. Methods Mol Med. 2004; 102:175–193. [PubMed: 15286386]
10. Neu N, Rose NR, Beisel KW, Herskowitz A, Gurri-Glass G, Craig SW. Cardiac myosin induces myocarditis in genetically predisposed mice. J Immunol. 1987; 139:3630–3636. [PubMed: 3680946]
11. Smith SC, Allen PM. Myosin-induced acute myocarditis is a T cell-mediated disease. J Immunol. 1991; 147:2141–2147. [PubMed: 1918949]
12. Weaver CT, Hatton RD, Mangan PR, Harrington LE. IL-17 family cytokines and the expanding diversity of effector T cell lineages. Annu Rev Immunol. 2007; 25:821–852. [PubMed: 17201677]
13. Baldeviano GC, Barin JG, Talor MV, Srinivasan S, Bedja D, Zheng D, Gabrielson K, Iwakura Y, Rose NR, Cihakova D. Interleukin-17A is dispensable for myocarditis but essential for the progression to dilated cardiomyopathy. Circ Res. 2010; 106:1646–1655. [PubMed: 20378858]
14. Kolls JK, Linden A. Interleukin-17 family members and inflammation. Immunity. 2004; 21:467–476. [PubMed: 15485625]
15. Iwakura Y, Ishigame H, Saijo S, Nakae S. Functional specialization of interleukin-17 family members. Immunity. 2011; 34:149–162. [PubMed: 21349428]
16. Gaffen SL. Structure and signalling in the IL-17 receptor family. Nature reviews Immunology. 2009; 9:556–567.
17. Harrington LE, Hatton RD, Mangan PR, Turner H, Murphy TL, Murphy KM, Weaver CT. Interleukin 17-producing CD4+ effector T cells develop via a lineage distinct from the T helper type 1 and 2 lineages. Nature immunology. 2005; 6:1123–1132. [PubMed: 16200070]
18. Park H, Li Z, Yang XO, Chang SH, Nurieva R, Wang YH, Wang Y, Hood L, Zhu Z, Tian Q, Dong C. A distinct lineage of CD4 T cells regulates tissue inflammation by producing interleukin 17. Nature immunology. 2005; 6:1133–1141. [PubMed: 16200068]
19. Veldhoen M, Hocking RJ, Atkins CJ, Locksley RM, Stockinger B. TGFbeta in the context of an inflammatory cytokine milieu supports de novo differentiation of IL-17-producing T cells. Immunity. 2006; 24:179–189. [PubMed: 16473830]
20. Ivanov, McKenzie BS, Zhou L, Tadokoro CE, Lepelley A, Lafaille JJ, Cua DJ, Littman DR. The orphan nuclear receptor RORgammat directs the differentiation program of proinflammatory IL-17+ T helper cells. Cell. 2006; 126:1121–1133. [PubMed: 16990136]
21. Bettelli E, Carrier Y, Gao W, Korn T, Strom TB, Oukka M, Weiner HL, Kuchroo VK. Reciprocal developmental pathways for the generation of pathogenic effector TH17 and regulatory T cells. Nature. 2006; 441:235–238. [PubMed: 16648838]
22. Luger D, Silver PB, Tang J, Cua D, Chen Z, Iwakura Y, Bowman EP, Sgambellone NM, Chan CC, Caspi RR. Either a Th17 or a Th1 effector response can drive autoimmunity: conditions of disease induction affect dominant effector category. J Exp Med. 2008; 205:799–810. [PubMed: 18391061]
23. Stummvoll GH, DiPaolo RJ, Huter EN, Davidson TS, Glass D, Ward JM, Shevach EM. Th1, Th2, and Th17 effector T cell-induced autoimmune gastritis differs in pathological pattern and in susceptibility to suppression by regulatory T cells. J Immunol. 2008; 181:1908–1916. [PubMed: 18641328]

NIH-PA Author Manuscript NIH-PA Author Manuscript NIH-PA Author Manuscript


24. Jager A, Dardalhon V, Sobel RA, Bettelli E, Kuchroo VK. Th1, Th17, and Th9 effector cells induce experimental autoimmune encephalomyelitis with different pathological phenotypes. J Immunol. 2009; 183:7169–7177. [PubMed: 19890056]
25. Eriksson U, Kurrer MO, Sebald W, Brombacher F, Kopf M. Dual role of the IL-12/IFN-gamma axis in the development of autoimmune myocarditis: induction by IL-12 and protection by IFN-gamma. J Immunol. 2001; 167:5464–5469. [PubMed: 11673566]
26. Afanasyeva M, Georgakopoulos D, Belardi DF, Bedja D, Fairweather D, Wang Y, Kaya Z, Gabrielson KL, Rodriguez ER, Caturegli P, Kass DA, Rose NR. Impaired up-regulation of CD25 on CD4+ T cells in IFN-gamma knockout mice is associated with progression of myocarditis to heart failure. Proc Natl Acad Sci U S A. 2005; 102:180–185. [PubMed: 15611472]
27. Afanasyeva M, Wang Y, Kaya Z, Stafford EA, Dohmen KM, Sadighi Akha AA, Rose NR. Interleukin-12 receptor/STAT4 signaling is required for the development of autoimmune myocarditis in mice by an interferon-gamma-independent pathway. Circulation. 2001; 104:3145–3151. [PubMed: 11748115]
28. Barin JG, Talor MV, Baldeviano GC, Kimura M, Rose NR, Cihakova D. Mechanisms of IFNgamma regulation of autoimmune myocarditis. Exp Mol Pathol. 2010; 89:83–91. [PubMed: 20599938]
29. Damsker JM, Hansen AM, Caspi RR. Th1 and Th17 cells: adversaries and collaborators. Ann N Y Acad Sci. 2010; 1183:211–221. [PubMed: 20146717]
30. Hu X, Ivashkiv LB. Cross-regulation of signaling pathways by interferon-gamma: implications for immune responses and autoimmune diseases. Immunity. 2009; 31:539–550. [PubMed: 19833085]
31. Berghmans N, Nuyts A, Uyttenhove C, Van Snick J, Opdenakker G, Heremans H. Interferon-gamma orchestrates the number and function of Th17 cells in experimental autoimmune encephalomyelitis. J Interferon Cytokine Res. 2011; 31:575–587. [PubMed: 21348780]
32. Qian X, Ning H, Zhang J, Hoft DF, Stumpo DJ, Blackshear PJ, Liu J. Posttranscriptional regulation of IL-23 expression by IFN-gamma through tristetraprolin. J Immunol. 2011; 186:6454–6464. [PubMed: 21515794]
33. Nakae S, Iwakura Y, Suto H, Galli SJ. Phenotypic differences between Th1 and Th17 cells and negative regulation of Th1 cell differentiation by IL-17. J Leukoc Biol. 2007; 81:1258–1268. [PubMed: 17307864]
34. Koike T. Interferon-gamma-independent suppression of Th17 cell differentiation by T-bet expression in mice with autoimmune arthritis. Arthritis Rheum. 2012; 64:40–41. [PubMed: 21905014]
35. Kelchtermans H, Schurgers E, Geboes L, Mitera T, Van Damme J, Van Snick J, Uyttenhove C, Matthys P. Effector mechanisms of interleukin-17 in collagen-induced arthritis in the absence of interferon-gamma and counteraction by interferon-gamma. Arthritis Res Ther. 2009; 11:R122. [PubMed: 19686583]
36. Nakae S, Komiyama Y, Nambu A, Sudo K, Iwase M, Homma I, Sekikawa K, Asano M, Iwakura Y. Antigen-specific T cell sensitization is impaired in IL-17-deficient mice, causing suppression of allergic cellular and humoral responses. Immunity. 2002; 17:375–387. [PubMed: 12354389]
37. Dalton DK, Pitts-Meek S, Keshav S, Figari IS, Bradley A, Stewart TA. Multiple defects of immune cell function in mice with disrupted interferon-gamma genes. Science. 1993; 259:1739–1742. [PubMed: 8456300]
38. Care, C.ftU.ot.Gf.t.,Uo.L. Animals, and N. R. Council. Guide for the Care and Use of Laboratory Animals: Eighth Edition. The National Academies Press; 2011.
39. Pummerer CL, Luze K, Grassl G, Bachmaier K, Offner F, Burrell SK, Lenz DM, Zamborelli TJ, Penninger JM, Neu N. Identification of cardiac myosin peptides capable of inducing autoimmune myocarditis in BALB/c mice. J Clin Invest. 1996; 97:2057–2062. [PubMed: 8621795]
40. Fairweather D, Stafford KA, Sung YK. Update on coxsackievirus B3 myocarditis. Current opinion in rheumatology. 2012; 24:401–407. [PubMed: 22488075]
41. Fairweather D, Rose NR. Coxsackievirus-induced myocarditis in mice: a model of autoimmune disease for studying immunotoxicity. Methods. 2007; 41:118–122. [PubMed: 17161308]
42. Livak KJ, Schmittgen TD. Analysis of relative gene expression data using real-time quantitative PCR and the 2(−Delta Delta C(T)) Method. Methods. 2001; 25:402–408. [PubMed: 11846609]

NIH-PA Author Manuscript

NIH-PA Author Manuscript

NIH-PA Author Manuscript


43. Edwards CA, O'Brien WD Jr. Modified assay for determination of hydroxyproline in a tissue hydrolyzate. Clinica chimica acta; international journal of clinical chemistry. 1980; 104:161–167.
44. Cihakova D, Barin JG, Afanasyeva M, Kimura M, Fairweather D, Berg M, Talor MV, Baldeviano GC, Frisancho S, Gabrielson K, Bedja D, Rose NR. Interleukin-13 protects against experimental autoimmune myocarditis by regulating macrophage differentiation. Am J Pathol. 2008; 172:1195–1208. [PubMed: 18403598]
45. Fairweather D, Frisancho-Kiss S, Rose NR. Viruses as adjuvants for autoimmunity: evidence from Coxsackievirus-induced myocarditis. Rev Med Virol. 2005; 15:17–27. [PubMed: 15386590]
46. Fairweather D, Kaya Z, Shellam GR, Lawson CM, Rose NR. From infection to autoimmunity. J Autoimmun. 2001; 16:175–186. [PubMed: 11334481]
47. Fairweather D, Frisancho-Kiss S, Yusung SA, Barrett MA, Davis SE, Steele RA, Gatewood SJ, Rose NR. IL-12 protects against coxsackievirus B3-induced myocarditis by increasing IFN-gamma and macrophage and neutrophil populations in the heart. J Immunol. 2005; 174:261–269. [PubMed: 15611248]
48. Fairweather D, Frisancho-Kiss S, Yusung SA, Barrett MA, Davis SE, Gatewood SJ, Njoku DB, Rose NR. Interferon-gamma protects against chronic viral myocarditis by reducing mast cell degranulation, fibrosis, and the profibrotic cytokines transforming growth factor-beta 1, interleukin-1 beta, and interleukin-4 in the heart. Am J Pathol. 2004; 165:1883–1894. [PubMed: 15579433]
49. Shinkai K, Mohrs M, Locksley RM. Helper T cells regulate type-2 innate immunity in vivo. Nature. 2002; 420:825–829. [PubMed: 12490951]
50. Rothenberg ME, Hogan SP. The eosinophil. Annu Rev Immunol. 2006; 24:147–174. [PubMed: 16551246]
51. Yu C, Cantor AB, Yang H, Browne C, Wells RA, Fujiwara Y, Orkin SH. Targeted deletion of a high-affinity GATA-binding site in the GATA-1 promoter leads to selective loss of the eosinophil lineage in vivo. J Exp Med. 2002; 195:1387–1395. [PubMed: 12045237]
52. O'Connor W Jr, Kamanaka M, Booth CJ, Town T, Nakae S, Iwakura Y, Kolls JK, Flavell RA. A protective function for interleukin 17A in T cell-mediated intestinal inflammation. Nat Immunol. 2009; 10:603–609. [PubMed: 19448631]
53. Ogawa A, Andoh A, Araki Y, Bamba T, Fujiyama Y. Neutralization of interleukin-17 aggravates dextran sulfate sodium-induced colitis in mice. Clin Immunol. 2004; 110:55–62. [PubMed: 14962796]
54. Kezic JM, Glant TT, Rosenbaum JT, Rosenzweig HL. Neutralization of IL-17 ameliorates uveitis but damages photoreceptors in a murine model of spondyloarthritis. Arthritis Res Ther. 2012; 14:R18. [PubMed: 22269151]
55. Veldhoen M, Hocking RJ, Flavell RA, Stockinger B. Signals mediated by transforming growth factor-beta initiate autoimmune encephalomyelitis, but chronic inflammation is needed to sustain disease. Nat Immunol. 2006; 7:1151–1156. [PubMed: 16998492]
56. Eriksson U, Kurrer MO, Bingisser R, Eugster HP, Saremaslani P, Follath F, Marsch S, Widmer U. Lethal autoimmune myocarditis in interferon-gamma receptor-deficient mice: enhanced disease severity by impaired inducible nitric oxide synthase induction. Circulation. 2001; 103:18–21. [PubMed: 11136679]
57. Mosmann TR, Coffman RL. TH1 and TH2 cells: different patterns of lymphokine secretion lead to different functional properties. Annu Rev Immunol. 1989; 7:145–173. [PubMed: 2523712]
58. Khan S, Orenstein SR. Eosinophilic gastroenteritis. Gastroenterology clinics of North America. 2008; 37:333–348. v. [PubMed: 18499023]
59. Nelson AM. Localized forms of scleroderma, including morphea, linear scleroderma, and eosinophilic fasciitis. Current opinion in rheumatology. 1996; 8:473–476. [PubMed: 8941452]
60. Alfadda AA, Storr MA, Shaffer EA. Eosinophilic colitis: an update on pathophysiology and treatment. British medical bulletin. 2011; 100:59–72. [PubMed: 22012125]
61. Afanasyeva M, Wang Y, Kaya Z, Park S, Zilliox MJ, Schofield BH, Hill SL, Rose NR. Experimental autoimmune myocarditis in A/J mice is an interleukin-4-dependent disease with a Th2 phenotype. Am J Pathol. 2001; 159:193–203. [PubMed: 11438466]

NIH-PA Author Manuscript

NIH-PA Author Manuscript

NIH-PA Author Manuscript


62. Abston ED, Barin JG, Cihakova D, Bucek A, Coronado MJ, Brandt JE, Bedja D, Kim JB, Georgakopoulos D, Gabrielson KL, Mitzner W, Fairweather D. IL-33 Independently Induces Eosinophilic Pericarditis and Cardiac Dilation: ST2 Improves Cardiac Function. Circulation Heart failure. 2012; 5:366–375. [PubMed: 22454393]
63. Cookston M, Stober M, Kayes SG. Eosinophilic myocarditis in CBA/J mice infected with Toxocara canis. Am J Pathol. 1990; 136:1137–1145. [PubMed: 2349964]
64. Schaffer SW, Dimayuga ER, Kayes SG. Development and characterization of a model of eosinophil-mediated cardiomyopathy in rats infected with Toxocara canis. Am J Physiol. 1992; 262:H1428–1434. [PubMed: 1317127]
65. Hirasawa M, Ito Y, Shibata MA, Otsuki Y. Mechanism of inflammation in murine eosinophilic myocarditis produced by adoptive transfer with ovalbumin challenge. Int Arch Allergy Immunol. 2007; 142:28–39. [PubMed: 17016056]
66. Endo Y, Iwamura C, Kuwahara M, Suzuki A, Sugaya K, Tumes DJ, Tokoyoda K, Hosokawa H, Yamashita M, Nakayama T. Eomesodermin Controls Interleukin-5 Production in Memory T Helper 2 Cells through Inhibition of Activity of the Transcription Factor GATA3. Immunity. 2011; 35:733–745. [PubMed: 22118525]
67. Rezaizadeh H, Sanchez-Ross M, Kaluski E, Klapholz M, Haider B, Gerula C. Acute eosinophilic myocarditis: diagnosis and treatment. Acute Card Care. 12:31–36. [PubMed: 20201659]
68. Al Ali AM, Straatman LP, Allard MF, Ignaszewski AP. Eosinophilic myocarditis: case series and review of literature. Can J Cardiol. 2006; 22:1233–1237. [PubMed: 17151774]
69. Cooper LT, Zehr KJ. Biventricular assist device placement and immunosuppression as therapy for necrotizing eosinophilic myocarditis. Nat Clin Pract Cardiovasc Med. 2005; 2:544–548. [PubMed: 16186853]
70. Roehrl MH, Alexander MP, Hammond SB, Ruzinova M, Wang JY, O'Hara CJ. Eosinophilic myocarditis in hypereosinophilic syndrome. Am J Hematol. 86:607–608. [PubMed: 21681785]
71. Gupta S, Markham DW, Drazner MH, Mammen PP. Fulminant myocarditis. Nat Clin Pract Cardiovasc Med. 2008; 5:693–706. [PubMed: 18797433]
72. Domingues HS, Mues M, Lassmann H, Wekerle H, Krishnamoorthy G. Functional and pathogenic differences of Th1 and Th17 cells in experimental autoimmune encephalomyelitis. PLoS One. 2010; 5:e15531. [PubMed: 21209700]
73. Codarri L, Gyulveszi G, Tosevski V, Hesske L, Fontana A, Magnenat L, Suter T, Becher B. RORgammat drives production of the cytokine GM-CSF in helper T cells, which is essential for the effector phase of autoimmune neuroinflammation. Nat Immunol. 12:560–567. [PubMed: 21516112]
74. Luna, L. Manual of Histologic Staining Methods of the Armed Forces Institute of Pathology. McGraw-Hill; New York, NY: 1968.

NIH-PA Author Manuscript
NIH-PA Author Manuscript
NIH-PA Author Manuscript



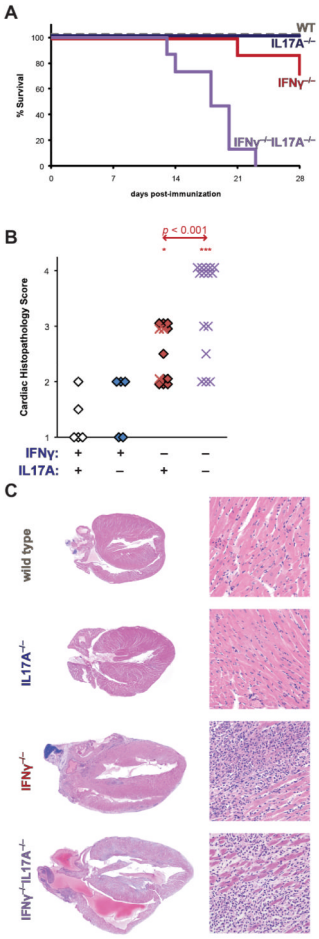


**Figure 1.**

IL17 accelerates lethal EAM on an IFNγ-deficient background. A) Survival of male IFNγ$^{-/-}$IL17A$^{-/-}$ (violet, *n* = 15), IFNγ$^{-/-}$ (red, *n* = 14), IL17A$^{-/-}$ (blue, *n* = 5), and wild type (grey, *n* = 5) mice during the first 28 days of EAM. B) Cardiac histopathology of IFNγ$^{-/-}$IL17A$^{-/-}$ (violet), IFNγ$^{-/-}$ (red), IL17A$^{-/-}$ (blue), and WT (open) mice at time of death from A. Prematurely expired mice from A are represented as crosses, whereas animals that survived to endpoint are depicted as diamonds. C) Representative histopathology from median animals of each group; staining by H&E, magnification at 2.5x (left) and 100x (right). Individual data points represent individual animals; bars indicate mean of each group.

NIH-PA Author Manuscript

NIH-PA Author Manuscript

NIH-PA Author Manuscript

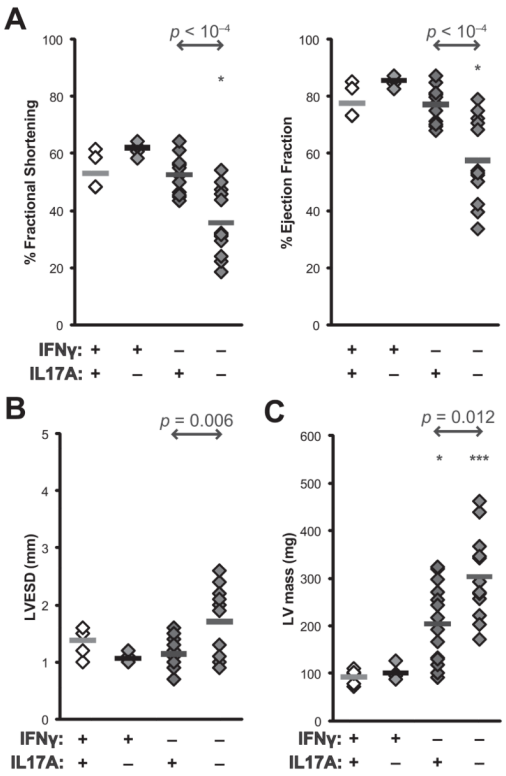


**Figure 2.**

IFNγ$^{-/-}$IL17A$^{-/-}$ mice rapidly develop inflammatory cardiomyopathy, as determined by echocardiographic imaging at day 14 of EAM. A) % fractional shortening (left) and % ejection fraction (right); B) Left-ventricular dimension at end-systole (LVESD); C) left ventricular mass in IFNγ$^{-/-}$IL17A$^{-/-}$, IFNγ$^{-/-}$, IL17A$^{-/-}$, and WT mice. Individual data points represent individual animals; bars indicate mean of each group.

NIH-PA Author Manuscript
NIH-PA Author Manuscript
NIH-PA Author Manuscript



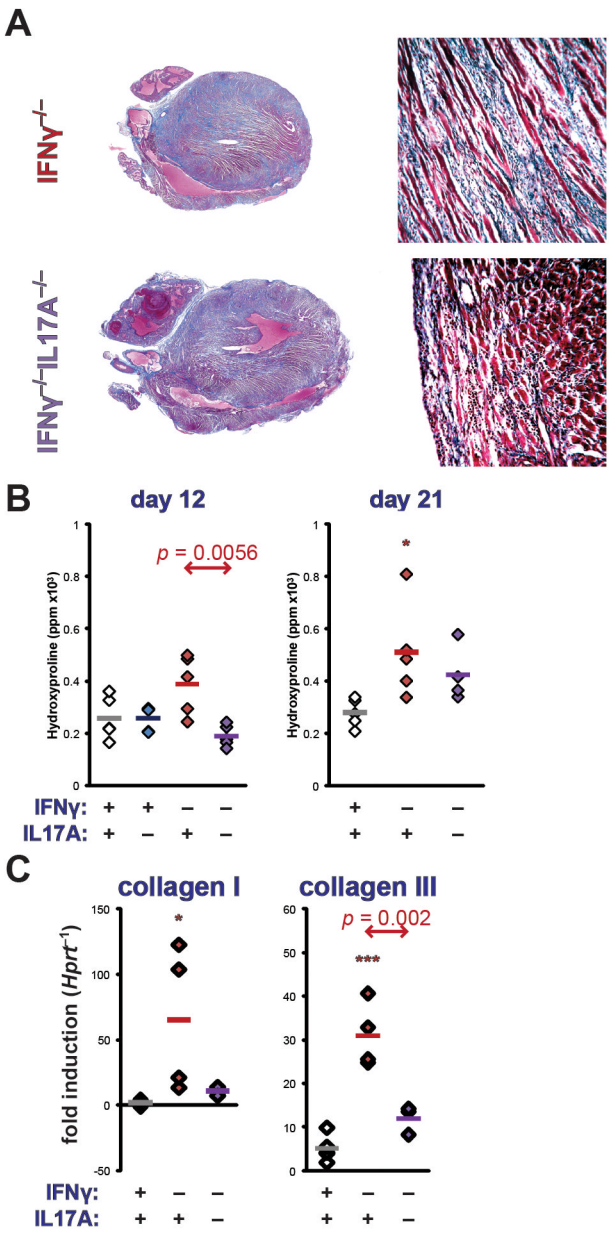


**Figure 3.**

Cardiac remodeling in the EAM of IFNγ$^{-/-}$IL17A$^{-/-}$ mice. A) Representative histopathology of IFNγ$^{-/-}$ (left) and IFNγ$^{-/-}$IL17A$^{-/-}$ (right) mice at day 21 of EAM, staining by Masson's Trichrome Blue, 2.5x (left) and 100x (right) magnification. B) Total cardiac hydroxyproline content on days 12 (left) and 21 (right) of EAM, normalized to heart weight, expressed as parts per million (ppm). C) Transcription of collagen I (*Col1a2*, left) and collagen III (*Col3a1*, right) at day 21 of EAM by realtime PCR. Individual data points represent individual animals; bars indicate mean of each group.

NIH-PA Author Manuscript
NIH-PA Author Manuscript
NIH-PA Author Manuscript



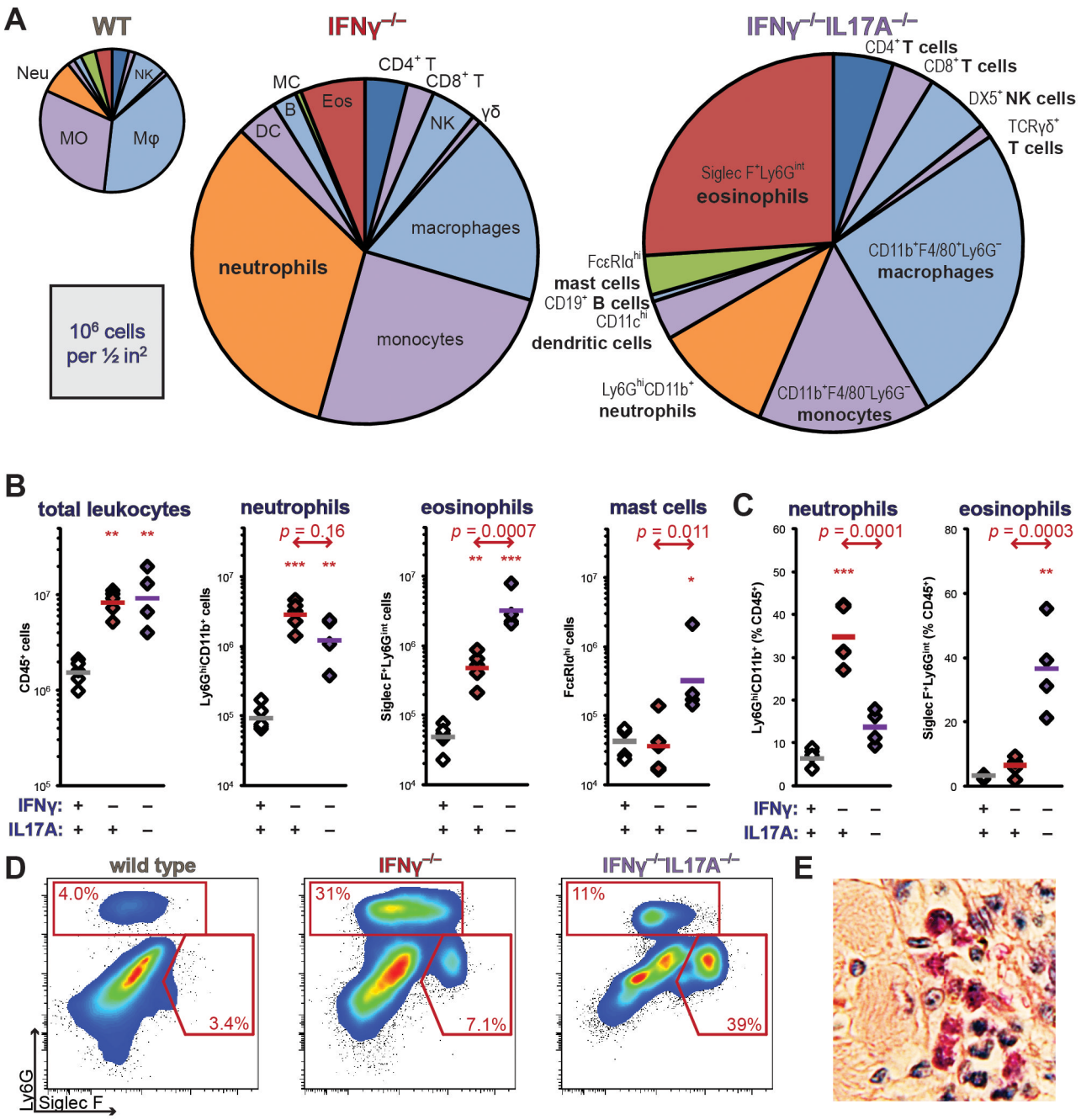


**Figure 4.**

Composition of inflammatory leukocytic cardiac infiltrates in IFNγ$^{-/-}$IL17A$^{-/-}$ mice at day 21 of EAM. A) Distribution of infiltrating inflammatory leukocytic populations as normalized means of groups; areas of pie graphs approximately correspond to absolute numbers. Notable populations are highlighted. B) Total intracardiac CD45$^{+}$ leukocytes, Ly6G$^{hi}$CD11b$^{+}$ neutrophils, Siglec F$^{+}$Ly6G$^{int}$ eosinophils, and FcεRIα$^{hi}$ mast cells expressed as absolute numbers; C) neutrophils and eosinophils expressed as a proportion of total CD45$^{+}$ leukocytes in WT, IFNγ$^{-/-}$, and IFNγ$^{-/-}$IL17A$^{-/-}$ mice. D) Representative bivariate gating of cardiac granulocytes, depicting median individual of each group. E) Representative cardiac eosinophil staining in an IFNγ$^{-/-}$IL17A$^{-/-}$ animal at day 21 of EAM,

by Verfuerth-Luna (74), 400x magnification. All cells are gated on viable $CD45^+$ events. Individual data points represent individual animals; bars indicate mean of each group.

NIH-PA Author Manuscript
NIH-PA Author Manuscript
NIH-PA Author Manuscript

NIH-PA Author Manuscript

NIH-PA Author Manuscript

NIH-PA Author Manuscript

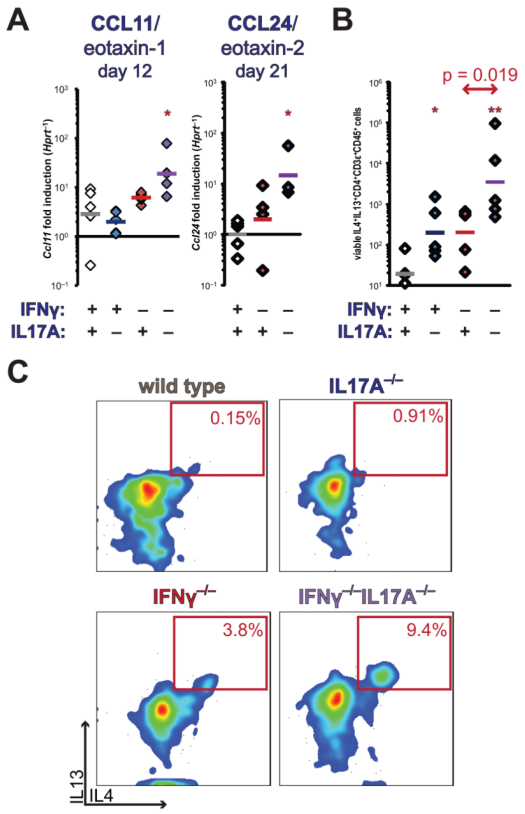


**Figure 5.**

Cardiac and spleen production of eosinotropic cytokines and chemokines. A) Cardiac transcription of CCL11/eotaxin-1 at day 12, and CCL24/eotaxin-2 at day 21 of EAM by realtime PCR. B) Absolute enumeration of heart-infiltrating $IL4^{+}IL13^{+}$ double-positive $CD4^{+}CD3\varepsilon^{+}$ Th2 cells at day 12 of EAM. C) Representative bivariate plots of IL4 and IL13 staining of viable intracardiac $CD4^{+}CD3\varepsilon^{+}CD45^{+}$-gated lymphocytes, depicting median individual of each group. Individual data points represent individual animals; bars indicate mean of each group.

NIH-PA Author Manuscript
NIH-PA Author Manuscript
NIH-PA Author Manuscript



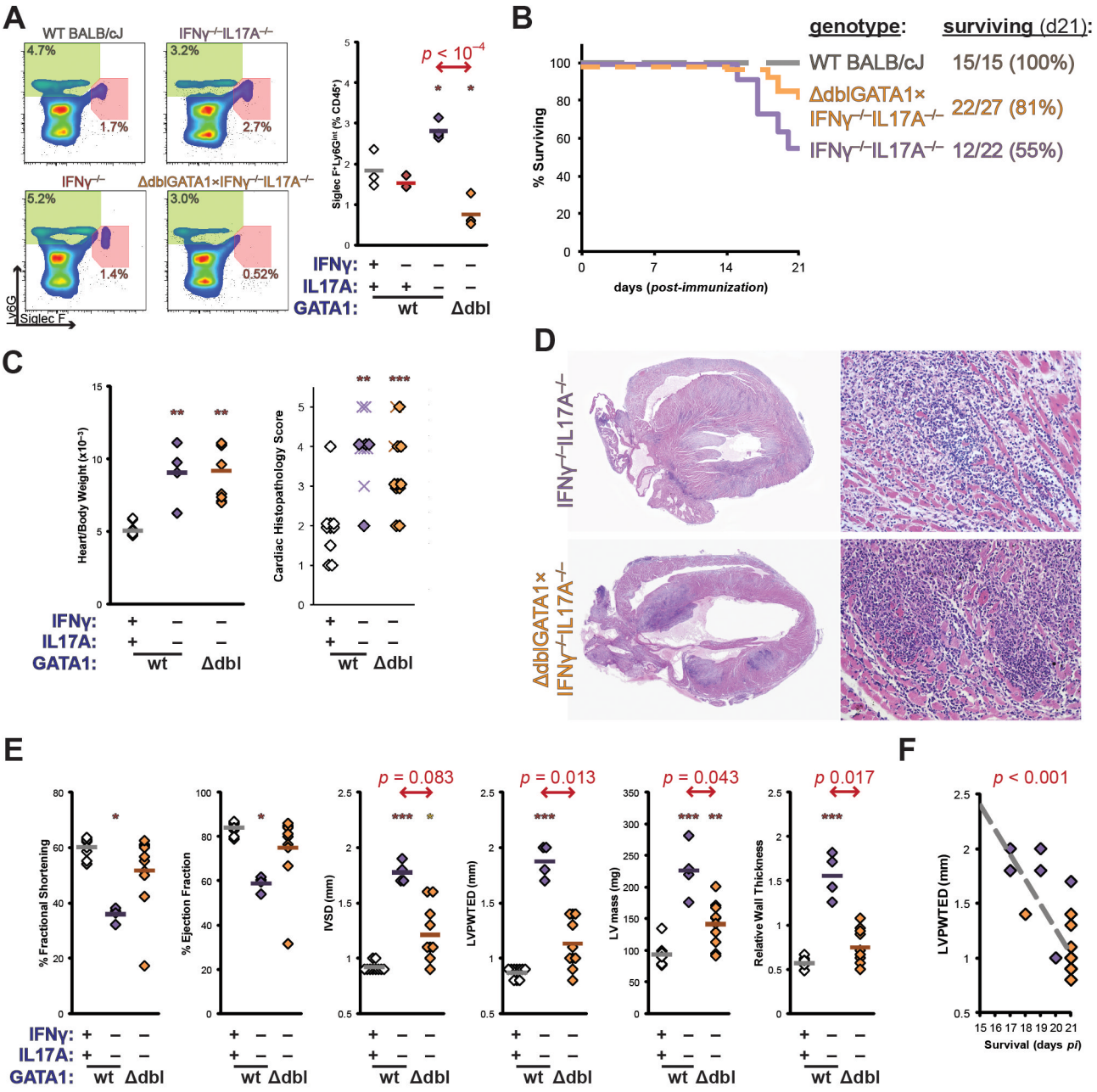


**Figure 6.**

Genetic ablation of eosinophil development reverses the mortality of IFNγ$^{-/-}$IL17A$^{-/-}$ mice. A) Established IFNγ$^{-/-}$IL17A$^{-/-}$ BALB/c mice were outcrossed to the ΔdblGATA1 BALB/c strain (JAX 5653), and resulting progeny intercrossed for a minimum of two generations to generate the homozygous triple-mutant founders depicted in representative bivariate plots of CD45$^{+}$-gated peripheral blood granulocytes from naïve ΔdblGATA1×IFNγ$^{-/-}$IL17A$^{-/-}$ mice (orange), and control strains; as well as quantitative analyses of Siglec F$^{+}$Ly6G$^{int}$ eosinophils. B) Survival of male IFNγ$^{-/-}$IL17A$^{-/-}$ (violet), WT BALB/c (grey, dashed), and ΔdblGATA1×IFNγ$^{-/-}$IL17A$^{-/-}$ mice (orange, dashed) mice during the first 21 days of EAM. Data represent a composite of two independent experiments. C) Relative heart weight at day 21 (left) and cardiac histopathology (right) of ΔdblGATA1×IFNγ$^{-/-}$IL17A$^{-/-}$ and

NIH-PA Author Manuscript

NIH-PA Author Manuscript

NIH-PA Author Manuscript

control mice at time of death. Prematurely expired mice from A are represented as crosses, whereas animals that survived to endpoint are depicted as diamonds. D) Representative histopathology of median individual animals; staining by H&E, magnification at 2.5x (left) and 100x (right). E) Echocardiographic imaging of ΔdblGATA1×IFNγ$^{-/-}$IL17A$^{-/-}$ and control mice on day 15 of EAM. F) Linear regressive correlation of LVPWTED and survival. Individual data points represent individual animals; bars indicate mean of each group.